British Journal of Pharmacology

British Journal of Pharmacology (2017) **174** 4383–4395 4383

RESEARCH PAPER

$G\alpha_{12}$ facilitates shortening in human airway smooth muscle by modulating phosphoinositide 3-kinase-mediated activation in a RhoA-dependent manner

Correspondence Reynold A Panettieri Jr, Rutgers Institute for Translational Medicine and Science, Child Health Institute, Rutgers University, 89 French Street, Room 4210, New Brunswick, NJ 08901, USA. E-mail: rp856@ca.rutgers.edu

Received 12 April 2017; **Revised** 12 September 2017; **Accepted** 12 September 2017

Edwin J Yoo[1,*], Gaoyuan Cao[1,*], Cynthia J Koziol-White[1], Christie A Ojiaku[1], Krishna Sunder[1], Joseph A Jude[1], James V Michael[2], Hong Lam[3], Ivan Pushkarsky[4], Robert Damoiseaux[5,6], Dino Di Carlo[4,6,7], Kwangmi Ahn[8], Steven S An[3,9], Raymond B Penn[2] and Reynold A Panettieri Jr[1]

[1]Rutgers Institute for Translational Medicine and Science, Child Health Institute, Rutgers University, New Brunswick, NJ, USA, [2]Department of Medicine, Division of Pulmonary and Critical Care Medicine, Center for Translational Medicine, Jane and Leonard Korman Lung Center, Thomas Jefferson University, Philadelphia, PA, USA, [3]Department of Environmental Health and Engineering, Johns Hopkins Bloomberg School of Public Health, Baltimore, MD, USA, [4]Department of Bioengineering, University of California, Los Angeles, CA, USA, [5]Department of Molecular and Medicinal Pharmacology, University of California, Los Angeles, CA, USA, [6]California NanoSystems Institute, University of California, Los Angeles, CA, USA, [7]Department of Mechanical Engineering, University of California, Los Angeles, CA, USA, [8]National Institute of Mental Health, Bethesda, MD, USA, and [9]Department of Chemical and Biomolecular Engineering, Johns Hopkins University, Baltimore, MD, USA

*Contributed equally as first author.

BACKGROUND AND PURPOSE

PI3K-dependent activation of Rho kinase (ROCK) is necessary for agonist-induced human airway smooth muscle cell (HASMC) contraction, and inhibition of PI3K promotes bronchodilation of human small airways. The mechanisms driving agonist-mediated PI3K/ROCK axis activation, however, remain unclear. Given that G_{12} family proteins activate ROCK pathways in other cell types, their role in M_3 muscarinic acetylcholine receptor-stimulated PI3K/ROCK activation and contraction was examined.

EXPERIMENTAL APPROACH

$G\alpha_{12}$ coupling was evaluated using co-immunoprecipitation and serum response element (SRE)-luciferase reporter assays. siRNA and pharmacological approaches, as well as overexpression of a regulator of G-protein signaling (RGS) proteins were applied in HASMCs. Phosphorylation levels of Akt, myosin phosphatase targeting subunit-1 (MYPT1), and myosin light chain-20 (MLC) were measured. Contraction and shortening were evaluated using magnetic twisting cytometry (MTC) and micro-pattern deformation, respectively. Human precision-cut lung slices (hPCLS) were utilized to evaluate bronchoconstriction.

KEY RESULTS

Knockdown of M_3 receptors or $G\alpha_{12}$ attenuated activation of Akt, MYPT1, and MLC phosphorylation. $G\alpha_{12}$ coimmunoprecipitated with M_3 receptors, and p115RhoGEF-RGS overexpression inhibited carbachol-mediated induction of SRE-luciferase reporter. p115RhoGEF-RGS overexpression inhibited carbachol-induced activation of Akt, HASMC contraction, and shortening. Moreover, inhibition of RhoA blunted activation of PI3K. Lastly, RhoA inhibitors induced dilation of hPCLS.

CONCLUSIONS AND IMPLICATIONS

$G\alpha_{12}$ plays a crucial role in HASMC contraction via RhoA-dependent activation of the PI3K/ROCK axis. Inhibition of RhoA activation induces bronchodilation in hPCLS, and targeting $G\alpha_{12}$ signaling may elucidate novel therapeutic targets in asthma. These findings provide alternative approaches to the clinical management of airway obstruction in asthma.

DOI:10.1111/bph.14040

Abbreviations

AHR, airway hyperresponsiveness; HASMCs, human airway smooth muscle cells; hTERT, human telomerase reverse transcriptase; MLC, myosin light chain; MLCP, myosin light chain phosphatase; MTC, magnetic twisting cytometry; PI3K, phosphoinositide 3-kinase; RGS, regulator of G-protein signalling; RhoGEF, Rho guanine nucleotide exchange factor; ROCK, Rho kinase

Introduction

Airway hyperresponsiveness (AHR), a hallmark of asthma, represents exaggerated airway narrowing in response to contractile agonists such as **carbachol** (Koziol-White and Panettieri, 2011; Panettieri, 2016). Human airway smooth muscle cells (HASMCs) mediate AHR by shortening in response to contractile agonists (Amrani *et al.*, 2004). Additionally, HASMCs are the primary target of bronchodilators, a cornerstone in the management of asthma (Black *et al.*, 2012).

Release of **ACh** from postganglionic parasympathetic nerves innervating the airway activates **M_3 muscarinic receptor**s, a class of GPCRs expressed in HASMCs (Billington and Penn, 2002). Stimulation of the M_3 receptors evokes $G\alpha_{q/11}$-mediated calcium release from the sarcoplasmic reticulum, resulting in myosin light chain (MLC) kinase activation and subsequent MLC phosphorylation. MLC phosphorylation induces actomyosin cross-bridge cycling and HASMC shortening (Billington and Penn, 2003). In parallel, activation of **Rho kinase** (ROCK) by the small GTPase RhoA phosphorylates and inactivates MLC phosphatase (MLCP). Inhibition of the constitutively active MLCP augments and sustains MLC phosphorylation and maintenance of HASMC contraction (Chiba and Misawa, 2004; Chiba *et al.*, 2010).

We recently demonstrated that **phosphoinositide 3-kinase** (PI3K), a lipid kinase, is a necessary mediator of muscarinic receptor-induced ROCK activation and human airway bronchoconstriction and that PI3K inhibitors can reverse carbachol-induced bronchoconstriction by attenuating the activation of the PI3K/ROCK-axis (Koziol-White *et al.*, 2016). The therapeutic importance of ROCK signalling is emphasized by the ability of ROCK and PI3K inhibitors to promote bronchodilation. The upstream mechanisms regulating muscarinic receptor-induced ROCK and PI3K activation in HASMC remain unclear and may provide insight into novel targets for asthma therapy (Pera and Penn, 2016).

$G\alpha_{12/13}$ family members, including $G\alpha_{12}$ and $G\alpha_{13}$, promote ROCK signalling by activating Rho guanine nucleotide exchange factors (RhoGEFs) including p115RhoGEF that exchange GDP for GTP and activate RhoA (Siehler, 2009). p115RhoGEF contains a regulator of **G-protein signalling (RGS)** domain that specifically limits $G\alpha_{12/13}$ signalling after activation (Wells *et al.*, 2002). $G\alpha_{12/13}$ proteins mediate various cell functions including stress fibre formation, cytoskeletal rearrangement and proliferation (Riobo and Manning, 2005; Worzfeld *et al.*, 2008). In the context of HASMC function, however, $G\alpha_{12/13}$ signalling remains poorly understood. In rodents, $G\alpha_{12/13}$ proteins contribute to AHR and have elevated expression upon allergen challenge (Chiba and Misawa, 2001; Lee *et al.*, 2009). HASMCs express multiple GPCRs that are known to couple to $G\alpha_{12/13}$ proteins, including **PAR**, **thromboxane (TP)** and EDG (**LPA** and **S1P**) receptors (Riobo and Manning, 2005). The M_3 receptor has also been shown to couple to $G\alpha_{12/13}$ proteins in HEK293 cells (Rümenapp *et al.*, 2001), but no studies in HASMCs have confirmed $G\alpha_{12/13}$ coupling to this receptor. Challenges in employing molecular approaches in primary cells, as well as the lack of pharmacological inhibitors against $G\alpha_{12/13}$ proteins, provide obstacles in characterizing the role of $G\alpha_{12/13}$ proteins in HASMC (Penn and Benovic, 2008).

In this study, we sought to determine the contribution of $G\alpha_{12/13}$ proteins in muscarinic receptor-induced PI3K/ROCK axis activation in HASMCs. To study the contribution of $G\alpha_{12/13}$ proteins in muscarinic receptor signalling, we used siRNA transfection in primary HASMCs and newly developed inhibitors that are highly specific to RhoA (Shang *et al.*, 2012). We also generated HASMC cell lines that overexpress the RGS domain of p115RhoGEF as an additional means of inhibiting $G\alpha_{12/13}$ signalling. Our data show that $G\alpha_{12}$ couples to the M_3 receptors in HASMCs and that $G\alpha_{12}$ plays an important role in facilitating HASMC shortening by promoting PI3K-mediated activation of ROCK in a RhoA-dependent manner.

Methods

Isolation and culture of HASMC

Human lungs were received from the National Disease Research Interchange (Philadelphia, PA, USA) and from the International Institute for the Advancement of Medicine (Edison, NJ, USA), and HASMCs were derived from the tracheas. All cell lines and tissue are obtained from de-identified donors, and their use does not constitute human subject research as described by the Rutgers Institutional Review Board. Culture of HASMCs was conducted as described previously (Panettieri *et al.*, 1989a). Briefly, cells were cultured in Ham's F-12 medium supplemented with 100 $U{\cdot}mL^{-1}$ penicillin, 0.1 $mg{\cdot}mL^{-1}$ streptomycin, 2.5 $mg{\cdot}mL^{-1}$ amphotericin B and 10% FBS. Medium was replaced every 72 h. HASMCs were only used during subculture passages 1–4 due to the strong expression of native contractile proteins (Panettieri *et al.*, 1989b). In studies using *Pertussis* toxin (PTX), cells were treated with 1 $\mu g{\cdot}mL^{-1}$ of PTX for 18 h. All pharmacological inhibitors were used with DMSO as the vehicle at a final concentration of 0.1% and were used to treat HASMC 30 min prior to agonist stimulation.

Retroviral infection

Stable expression of GFP and p115RhogefRGS-GFP was achieved by retroviral infection as described previously (Kong *et al.*, 2008; Deshpande *et al.*, 2014). Briefly, retrovirus for the expression of each construct was produced by cotransfecting GP2-293 cells with pVSV-G vector [encoding the pantropic (VSV-G) envelope protein] and pLPCX-GFP or pLPCX-p115RhogefRGS-GFP. Forty-eight hours after transfection,

supernatants were harvested and used to infect human telomerase reverse transcriptase (hTERT) immortalized airway smooth muscle cultures, with effective virus concentrations established by immunoblot analysis. Cultures were selected to homogeneity with 1 $\mu g \cdot mL^{-1}$ puromycin as described previously (Kong *et al.*, 2008; Deshpande *et al.*, 2014).

Generation of hPCLS and airway dilation assays

Human precision-cut lung slices (hPCLSs) were prepared as previously described (Cooper *et al.*, 2009). Briefly, human lungs were dissected and filled with 2% ($w \cdot v^{-1}$) low melting point agarose. After the agarose had solidified, the lobe was sectioned, and 8 mm diameter cores were generated. Cores containing small airways were sliced at a thickness of 350 μM using Precisionary Instruments VF300 Vibratome. They were then collected in supplemented Ham's F-12 medium. Generated slices came from all areas of the lung and not just one specific area. Airways from each core were randomized to the different treatment groups prior to the start of the experiment. Airways were constricted with a range of concentrations carbachol (10^{-8}–10^{-5} M), then dilated with one of the following agents (10^{-11}–10^{-4} M): diluent (DMSO), formoterol or the Rho inhibitor, Rhosin (Shang *et al.*, 2012). DMSO alone did not induce airway dilation at the concentrations tested (data not shown).

To assess luminal area, lung slices were placed in a 12-well plate in media and held in place using a platinum weight with nylon attachments. The airway was located using a microscope (Nikon Eclipse; model no. TE2000-U; magnification, ×40) connected to a live video feed (Evolution QEi; model no. 32-0074A-130 video recorder). Airway luminal area was measured using Image-Pro Plus software (version 6.0; Media Cybernetics, Rockville, MD, USA) and represented in mm^2 (Cooper *et al.*, 2009). After functional studies, the area of each airway at baseline and after drug incubation (receptor agonists, 5min; intracellular inhibitors, 30min) was calculated using Image-Pro Plus software. Maximal effect of drug (E_{max}), log of the concentration to induce 50% of maximal drug effect (log EC_{50}) and the AUC were calculated from the concentration–response curves. Airway dilation was calculated as % reversal of maximal bronchoconstriction and expressed as % forskolin response after normalizing to forskolin stimulation (10 μM).

siRNA transfection

Ham's F-12 media, DharmaFECT 1 reagent and siRNA were combined in a microcentrifuge tube according to the manufacturer's protocol and incubated for 20 min. HASMCs were trypsinized, and trypsin was inactivated with 5% FBS. Cells were centrifuged and resuspended in Ham's F-12 media. Cell suspension was added to the siRNA mixture and incubated for 15 min. The cell suspension and the siRNA mixture were then seeded into cell culture plates according to experimental design and incubated for 6 h. After 6 h, complete cell culture media (described above) were added to the cell culture plate wells in a 1:1 ratio and were incubated for 18 h. After 18 h, media were changed to complete media. Cells were serum deprived for 24 h before collection. Cells were collected 72 h post-transfection.

cAMP assay

HASMCs were seeded in a 24-well plate until about 80% confluent and serum deprived overnight. Cells were stimulated and lysed using cAMP-Screen System ELISA from Applied Biosystems (Bedford, MA, USA). Experiments were conducted according to the manufacturer's protocol.

SRE-luciferase assay

HASMCs were seeded and grown to 75% confluence. Complete medium was removed, and Cignal Lenti Serum Response Element (SRE) Reporter (CLS-010L-1) was added to cells with SureENTRY Transduction reagent (336921), according to the manufacturer's protocol. After 24 h, media were changed to complete medium. After 24 h, media were changed to serum-free media. Following 48 h incubation in serum-free media, cells were stimulated with carbachol for 6 h and collected with luciferase lysis buffer (E1483) from Promega (Madison, WI, USA).

Immunoblot analysis

After transfection with siRNA or incubation with pharmacological inhibitors, cells were stimulated with carbachol (10 μM–10 min). Perchloric acid was added to cell media to attain a final concentration of 0.1%. Cells were scraped, collected and pelleted. Pellets were washed once with ice-cold PBS. PBS was aspirated, and pellets were solubilized in RIPA. Sample buffer was added, and samples were subjected to SDS-PAGE and transferred to nitrocellulose membranes, as previously described (Balenga *et al.*, 2015; Koziol-White *et al.*, 2016). Phosphorylation of MYPT1, MLC and Akt were assessed, and band densities were normalized to GAPDH, total MYPT1, total MLC or total Akt band density.

Co-immunoprecipitation

After stimulation, HASMCs grown on 10 cm plates were lysed using ice-cold cell lysis buffer from Cell Signaling Technology containing 1% Triton X-100 with protease and phosphatase inhibitors from Thermo Fisher Scientific (Waltham, MA, USA). Lysate was incubated with primary antibody and incubated overnight with gentle rocking at 4°C. Protein A was incubated with lysates with gentle rocking for 3 h at 4°C. Samples were microcentrifuged for 30 s at 4°C and the pellet was washed five times with cell lysis buffer. The pellet was resuspended with SDS sample buffer and heated for 10 min at 70°C. The sample was then loaded onto SDS-PAGE gel and analysed by immunoblot.

Magnetic twisting cytometry (MTC)

Dynamic changes in cell stiffness were measured in isolated HASMCs using forced motions of functionalized beads anchored to the cytoskeleton through cell surface integrin receptors, as previously described in detail (Fabry *et al.*, 2001; An *et al.*, 2006; Deshpande *et al.*, 2015). The increase or decrease in stiffness is considered an index of single-cell smooth muscle contraction and relaxation respectively. For these studies, serum-deprived, post-confluent cultured HASMCs were plated at 30 000 cells per cm^2 on plastic wells (96-well Removawell, Immulon II; Dynatec Labs, El Paso, TX, USA) previously coated with type I collagen (VitroCol; Advanced BioMatrix, Inc., San Diego, CA, USA) at 500 $ng \cdot cm^{-2}$ and

maintained in serum-free media for 24 h at 37°C in humidified air containing 5% CO_2. These conditions have been optimized for seeding cultured cells on collagen matrix and for assessing their mechanical properties. For each individual cell, the baseline stiffness was measured for the first 60 s, and after drug addition, the stiffness was measured continuously for the next 14 min. Drug-induced changes in cell stiffness approached a steady-state level by 15 min. Agonist-induced contraction was normalized to baseline contraction and expressed as % over basal.

Micro-pattern deformation

Soft silicone elastomer films were micro-patterned with fibronectin and fluorescent fibrinogen in uniform 'X' shapes (70 μm diagonal by 10 μm thick) as previously described (Tseng *et al.*, 2014; Koziol-White *et al.*, 2016). The non-patterned regions were blocked using 0.5% Pluronic F-127, inhibiting cellular adhesion away from the fibronectin patterns. Isolated cells adhering to these 'X'-shaped micropatterns exerted traction forces causing deformations of the micro-patterns. Dimensions of contracted micro-patterns, which correspond directly to the force applied on them by adhered cells, relative to the original unperturbed dimensions were used to assess cellular contractile responses to carbachol. Prior to stimulation, cells were seeded into a 96-well plate functionalized with the described micro-patterned elastomeric film (into 36 wells each), allowed to adhere and serum-starved for 24 h. At the time of the experiment, cells were imaged at baseline, treated with carbachol (30 μM) and imaged at five 6 min intervals, then treated with bradykinin (10^{-5} M) and imaged for an additional four 6 min intervals. Cell nuclei were stained with Hoechst 33342 prior to imaging, and only the patterns co-localized with exactly one stained nucleus were used in the analysis. Following these studies, MATLAB was used to measure each individual pattern occupied by a single cell at each interval. Using an additional automated script, each population was mined for 'responder' cells, defined as the individual cells that exhibited at least a 25% contractile increase over baseline at their peak response to bradykinin (which acts *via* an orthogonal pathway to carbachol). The contractile activity to carbachol was compared among such responders from each group.

Data and statistical analysis

The data and statistical analysis comply with the recommendations on experimental design and analysis in pharmacology (Curtis *et al.*, 2015). Each experimental condition or vehicle condition (stock media) was normalized to an unstimulated condition (basal) within each experiment and expressed as fold x basal. The normalized values for each condition were then tested for normal distribution using the Shapiro–Wilk normality test using a threshold of $P = 0.05$. GraphPad Prism software (graph pad., La Jolla, CA, USA) was used to determine statistical significance evaluated by Student's unpaired *t*-test for two groups or ANOVA with Bonferroni's post test for three or more groups. P values <0.05 were considered significant. For single-cell shortening data, cells were not compared with themselves for each treatment group, so repeated measures analysis was not used. Data were normally distributed, and ANOVAs were used for data analysis, with Bonferroni's post test. Differences were isolated using the Bonferroni's post test for all pairwise comparisons. For MTC, agonist-induced contraction normalized to baseline contraction data were normally distributed and analysed by Student's two-tailed *t*-tests. SigmaStat (Systat, San Jose, CA, USA) and GraphPad Prism software were used in statistical analyses.

Materials

CHRM2 (L-005463-01-0005), CHRM3 (L-005464-00-0005), NT siRNA (D-001810-10-05), GNA12 (L-008435-00-0005), GNA13 (L-009948-00-0005), RhoA (L-003860-00-0005) and Rac1 (L-003560-00-0005) siRNA were obtained from Dharmacon (Lafayette, CO, USA). Carbachol (carbamoyl choline chloride), **formoterol** (formoterol fumarate dihydrate), **isoprenaline** (isoproterenol hydrochloride), **bradykinin** (bradykinin acetate salt), *Pertussis* toxin (PTX) and perchloric acid were purchased from Sigma-Aldrich (St. Louis, MO, USA). Rhosin (555460) was purchased from EMD Millipore (Darmstadt, Germany). Antibodies for detection of pMYPT1-Thr^{696} (5163S), pAkt (4060S), pMLC (3674S) and GAPDH (2118S) and total Akt (4691S) were purchased from Cell Signaling Technology (Danvers, MA, USA). Antibodies for immunoprecipitation and detection of M_3 receptors (SC-9108) and $G\alpha_{12}$ (SC-409) were obtained from Santa Cruz Biotechnology (Dallas, TX, USA). Total MLC antibody (MABT180) was obtained from EMD Millipore. Total MYPT1 antibody (612165) was obtained from BD Biosciences (San Jose, CA, USA).

Nomenclature of targets and ligands

Key protein targets and ligands in this article are hyperlinked to corresponding entries in http://www.guidetopharmacology.org, the common portal for data from the IUPHAR/BPS Guide to PHARMACOLOGY (Southan *et al.*, 2016), and are permanently archived in the Concise Guide to PHARMACOLOGY 2015/16 (Alexander *et al.*, 2015a,b,c).

Results

The muscarinic M_3 receptor, but not the M_2 receptor, mediates carbachol-induced Akt and MLC phosphorylation

Both the M_2 and M_3 muscarinic receptor subtypes are expressed in HASMCs (Billington and Penn, 2002). In order to determine the receptor(s) contributing to carbachol-mediated activation of PI3K/ROCK axis, we examined the effects of carbachol stimulation (10 μM, 10 min) on **Akt** (S473) and MLC (S19) phosphorylation in primary HASMCs 72 h after transfection with siRNA for the **M_2 receptor** or the M_3 receptor or a scrambled siRNA. Immunoblot analysis confirmed that the siRNA for M_3 receptors reduced the expression of this protein (Figure 1A), whereas M_2 receptor knockdown was confirmed by quantitative PCR. M_3 receptor siRNA attenuated carbachol-induced phosphorylation of Akt and phosphorylation of MLC, compared with scrambled siRNA (Figure 1B, C). The siRNA for M_2 receptors had little effect on carbachol-induced MLC phosphorylation when compared with scrambled siRNA. Surprisingly, the M_2 receptor siRNA induced Akt phosphorylation in the absence of

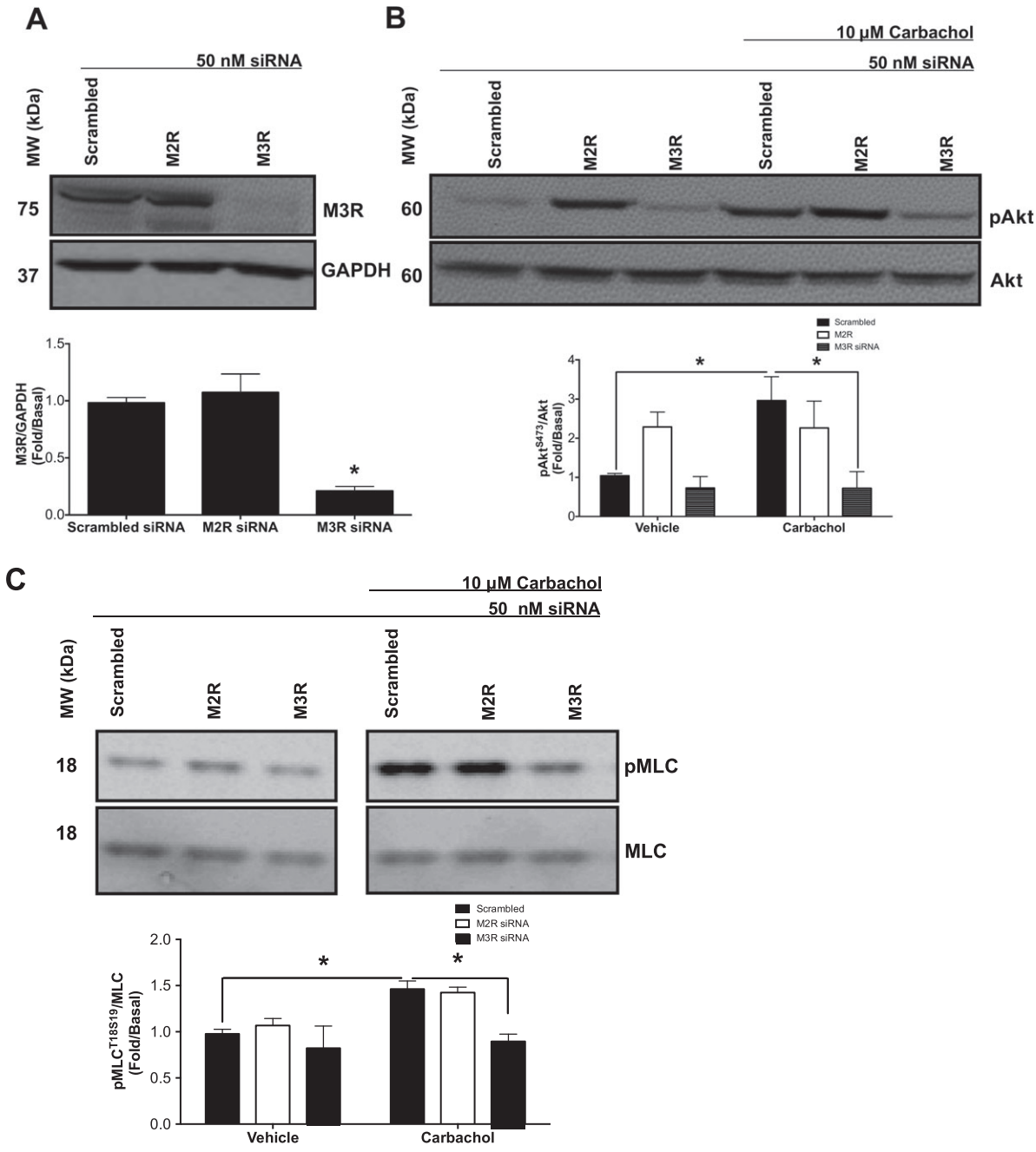

Figure 1

Effects of M_2 receptor siRNA, M_3 receptor siRNA and PTX on carbachol-induced Akt and MLC phosphorylation in primary HASMCs. (A–C) Measurement of phosphorylation responses to carbachol (10 μM, 10 min) and protein expression in primary HASMCs after transfection with M_2 receptor, M_3 receptor or scrambled siRNA (50 nM, 72 h post-transfection). (A) Effect of scrambled, M_2 receptor and M_3 receptor siRNA on protein expression. Data normalized to GAPDH expression in the same samples. (B) Effect of carbachol on Akt phosphorylation at S473 (pAkt) after transfection with scrambled, M_2 receptor and M_3 receptor siRNA. pAkt data were normalized to total Akt (Akt). (C) Effect of carbachol on MLC phosphorylation at S19 (pMLC) after transfection with scrambled, M_2 receptor and M_3 receptor siRNA. pMLC data were normalized to total MLC (MLC). (D) Effect of PTX (18 h, 1 $\mu g \cdot mL^{-1}$) on carbachol-induced Akt phosphorylation. Data normalized to tubulin expression in the same samples. (E) Effect of PTX (18 h, 1 $\mu g \cdot mL^{-1}$) on carbachol-induced attenuation of isoprenaline-mediated cAMP production. Data are expressed as fold change over untreated (basal) samples that were measured on the same gel or plate. Data (means ± SD) are from five independent experiments ($n = 5$). *$P < 0.05$, significantly different as indicated; one-way ANOVA with Bonferroni's post test. n.s., not significant.

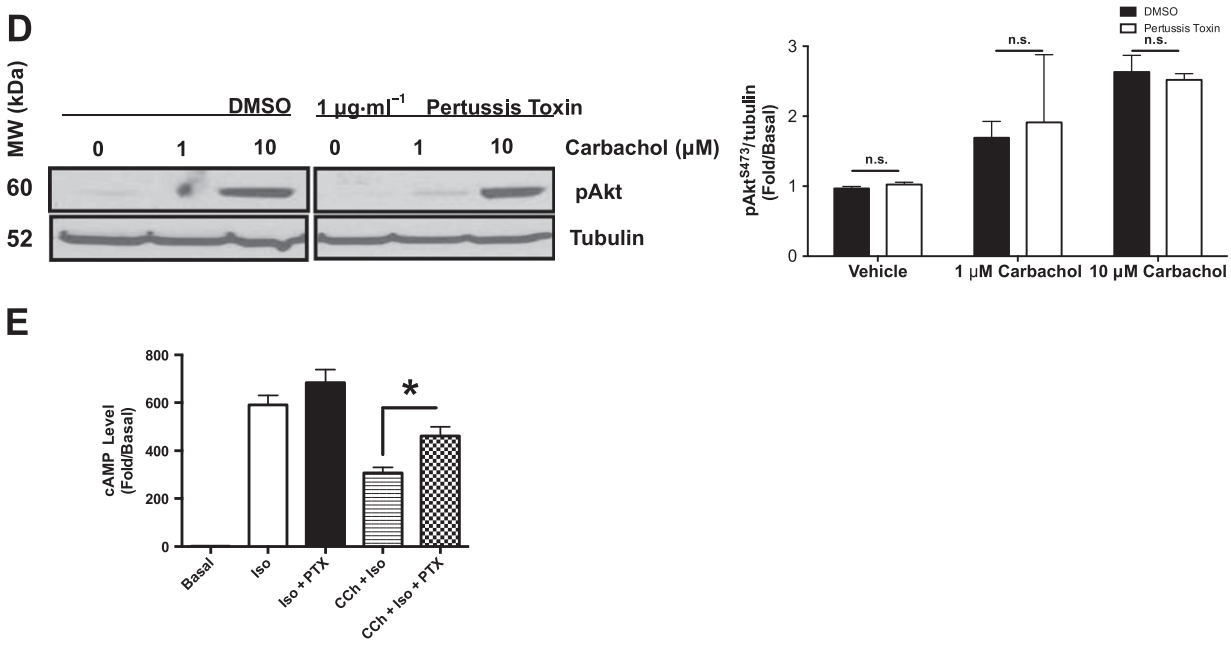

Figure 1
(Continued)

agonist. Because the M_2 receptor couples predominantly to the G protein $G\alpha_i$, we used PTX (18 h, 1 μg·mL^{-1}) to ADP-ribosylate $G\alpha_i$, rendering it inactive, and measured Akt phosphorylation in response to carbachol stimulation (10 μM, 10 min). Incubation with PTX before carbachol stimulation had little effect on Akt phosphorylation when compared with vehicle (0.01% DMSO) (Figure 1D), yet rescued carbachol-induced attenuation of isoprenaline-mediated cAMP elevation (Figure 1E), suggesting the effect of M_2 receptor knockdown was independent of any reduction in M_2 receptor activation of $G\alpha_i$.

$G\alpha_{12}$ couples to the M_3 receptors in HASMCs

Previous reports using HEK293 cells with GTP photolabelling and $G\alpha_{12}$-specific RGS overexpression have demonstrated that $G\alpha_{12}$ is coupled to M_3 receptors (Rümenapp *et al.*, 2001; Riobo and Manning, 2005). To determine whether similar coupling occurs in HASMCs, we used co-immunoprecipitation techniques to pull down the M_3 receptor and $G\alpha_{12}$ proteins. These samples were subsequently immunoblotted for the indicated proteins (Figure 2A). When the M_3 receptors were immunoprecipitated and subsequently probed with $G\alpha_{12}$ antibody, a strong band was present for $G\alpha_{12}$ (Supporting Information Figure S1). In HASMCs subject to carbachol stimulation (10 μM, 1 min), the band density diminished. Interestingly, when $G\alpha_{12}$ was immunoprecipitated and subsequently immunoblotted using the M_3 receptor antibody, a strong band was also present. Again, band density diminished under conditions of carbachol stimulation. To further evaluate M_3 receptor-$G\alpha_{12}$ coupling, hTERT-immortalized HASMCs overexpressing a GFP-tagged RGS domain of the p115RhoGEF enzyme (p115RhoGEF-RGS-GFP) were infected with an SRE-luciferase reporter construct that induces luciferase expression upon $G\alpha_{12}$ activation. These cells were stimulated with carbachol (10 μM, 6 h), lysed and assayed for luciferase induction using luminescence. Carbachol stimulation elevated luciferase expression almost two-fold (Figure 2B). Carbachol-induced luciferase induction was reduced to basal levels in HASMCs expressing p115RhoGEF-RGS, suggesting the effective inhibition of $G\alpha_{12}$ signalling by p115RhoGEF-RGS-GFP (Figure 2B).

$G\alpha_{12}$ mediates M_3 receptor-induced activation of PI3K/ROCK axis

To determine the contribution of $G\alpha_{12}$ proteins to the activation of the PI3K/ROCK axis, induced by carbachol, we used siRNA to knockdown $G\alpha_{12}$ proteins and measured the effects on carbachol-induced (10 μM, 10 min) phosphorylation of Akt, MYPT1 and MLC in primary HASMCs 72 h after transfection with $G\alpha_{12}$ proteins or scrambled siRNA. $G\alpha_{12}$ siRNA knockdown reduced $G\alpha_{12}$ protein expression (Figure 3A), and scrambled siRNA had little effect on any of the proteins examined. $G\alpha_{12}$ siRNA markedly attenuated carbachol-induced phosphorylation of Akt, MYPT1 and MLC, compared with scrambled siRNA (Figure 3B). To complement the $G\alpha_{12}$ siRNA studies, we compared carbachol-induced Akt phosphorylation and contraction in hTERT-immortalized HASMC that do or do not express p115RhoGEF-RGS. In p115RhoGEF-RGS-expressing HASMCs, carbachol-induced Akt phosphorylation was attenuated compared with control cell lines (Figure 3C). p115RhoGEF-RGS expression had little effect on $G\alpha_q$ activation, measured by intracellular calcium mobilization (Figure 3D). Carbachol-induced contraction and shortening were also attenuated compared with control cell lines (Figure 3E, G).

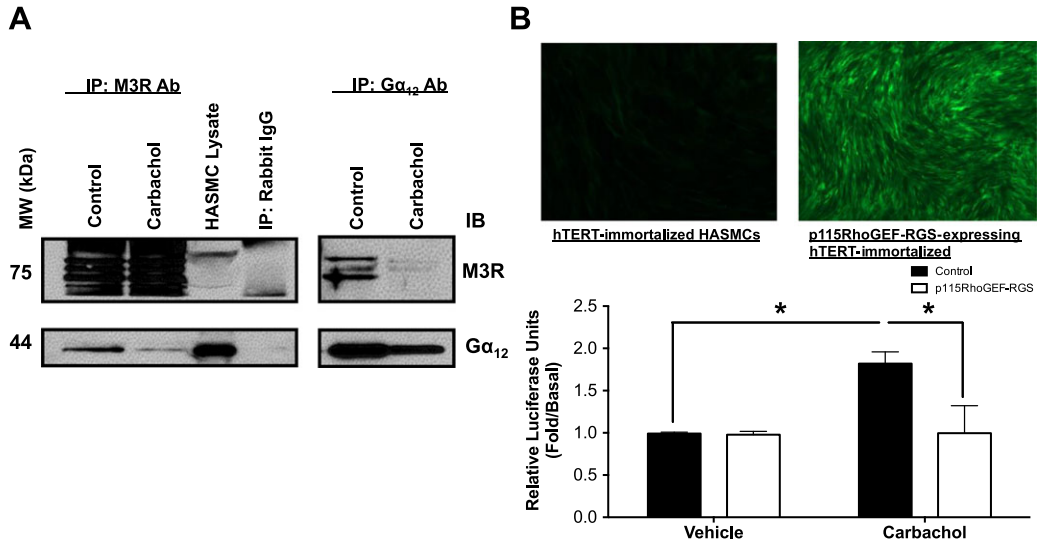

Figure 2

$G\alpha_{12}$ and M_3 receptor coupling in HASMCs. Evaluation of M_3 receptor-$G\alpha_{12}$ coupling using co-immunoprecipitation in primary HASMCs and SRE-luciferase reporter in hTERT-immortalized HASMCs expressing p115RhoGEF-RGS. (A) HASMCs were stimulated with carbachol (10 μM, 1 min), and lysates were immunoprecipitated with anti- M_3 receptor or anti-$G\alpha_{12}$ antibody and then probed as indicated. Immunoblot is representative of five independent experiments. (B) hTERT-immortalized HASMCs expressing p115RhoGEF-RGS and control hTERT-immortalized HASMCs (post-G418 selection) were infected with SRE-luciferase reporter. After carbachol stimulation (10 μM, 6 h), cells were lysed, and SRE-luciferase reporter activity was measured. Data are expressed as fold change over untreated (basal) samples that were measured on the same plate. Data (means ± SD) are from six independent experiments ($n = 6$), *$P < 0.05$, significantly different as indicated; one-way ANOVA with Bonferroni's post test.

$G\alpha_{12}$-mediated activation of PI3K is RhoA dependent

Although our previous studies implicated PI3K in the activation of ROCK by carbachol, the potential for Rho family GTPases to regulate PI3K isoforms has been previously suggested (Yang *et al.*, 2012). In order to determine whether $G\alpha_{12}$-mediated activation of PI3K involved Rho and Rac small GTPases as signalling intermediates, we examined the effects of carbachol stimulation (10 μM, 10 min) on Akt (S473) phosphorylation in primary HASMCs 72 h after transfection with RhoA, Rac1 or scrambled siRNA. RhoA and Rac1 siRNA knockdown reduced protein expression to a similar extent (Figure 4A), and scrambled siRNA had little effect on any of the proteins examined. RhoA siRNA attenuated carbachol-induced phosphorylation of Akt , compared with scrambled siRNA (Figure 4B). To complement siRNA studies, we next used Rhosin to inhibit RhoGEFs that activate RhoA and measured Akt phosphorylation in response to carbachol stimulation. Incubation with Rhosin attenuated carbachol-induced phosphorylation of Akt, compared with vehicle (Figure 4C). These results suggest that RhoA either functions upstream of PI3K or modulates activation of PI3K through cooperativity.

RhoA inhibition promotes bronchodilation of hPCLS

To determine if inhibition of RhoA could reverse agonist-induced bronchoconstriction, hPCLSs were stimulated with carbachol to induce luminal narrowing and subsequently treated with increasing doses of Rhosin or formoterol to evaluate airway dilation (Figure 5). Formoterol reversed carbachol-induced bronchoconstriction with an E_{max} of 100 ± 3% and log EC_{50} of −6.3.

Discussion

Our study demonstrates a previously unidentified role for $G\alpha_{12}$ in the modulation, by M_3 receptors, of the activation of the PI3K/ROCK axis in HASMCs. We also demonstrate that $G\alpha_{12}$-mediated activation of PI3K/ROCK axis is RhoA dependent. Furthermore, we show that inhibition of RhoA blunts carbachol-induced PI3K activation and promotes bronchodilation of human small airways, implicating RhoA as a pivotal mediator of airway tone.

To expand on our previous studies demonstrating that PI3K inhibitors promote bronchodilation of human small airways, we sought to delineate upstream signalling pathways that mediate PI3K activation. We used siRNA and pharmacological tools, as well as HASMCs overexpressing p115RhoGEF-RGS proteins that inhibit M_3 receptor-mediated activation of $G\alpha_{12}$, in order to determine the role of $G\alpha_{12}$ in modulating PI3K/ROCK axis activation and HASMC contraction. Our data showed that knockdown of M_3 receptors attenuated carbachol-induced activation of Akt, MYPT1 and MLC phosphorylation. We also showed that $G\alpha_{12}$ co-immunoprecipitated with M_3 receptors and that p115RhoGEF-RGS expression inhibited carbachol-mediated induction of SRE-luciferase reporter. $G\alpha_{12}$ siRNA attenuated carbachol-induced activation of Akt, MYPT1 and MLC phosphorylation, and p115RhoGEF-RGS overexpression similarly reduced carbachol-induced activation of Akt and HASM contraction. Furthermore, we demonstrated that siRNA and

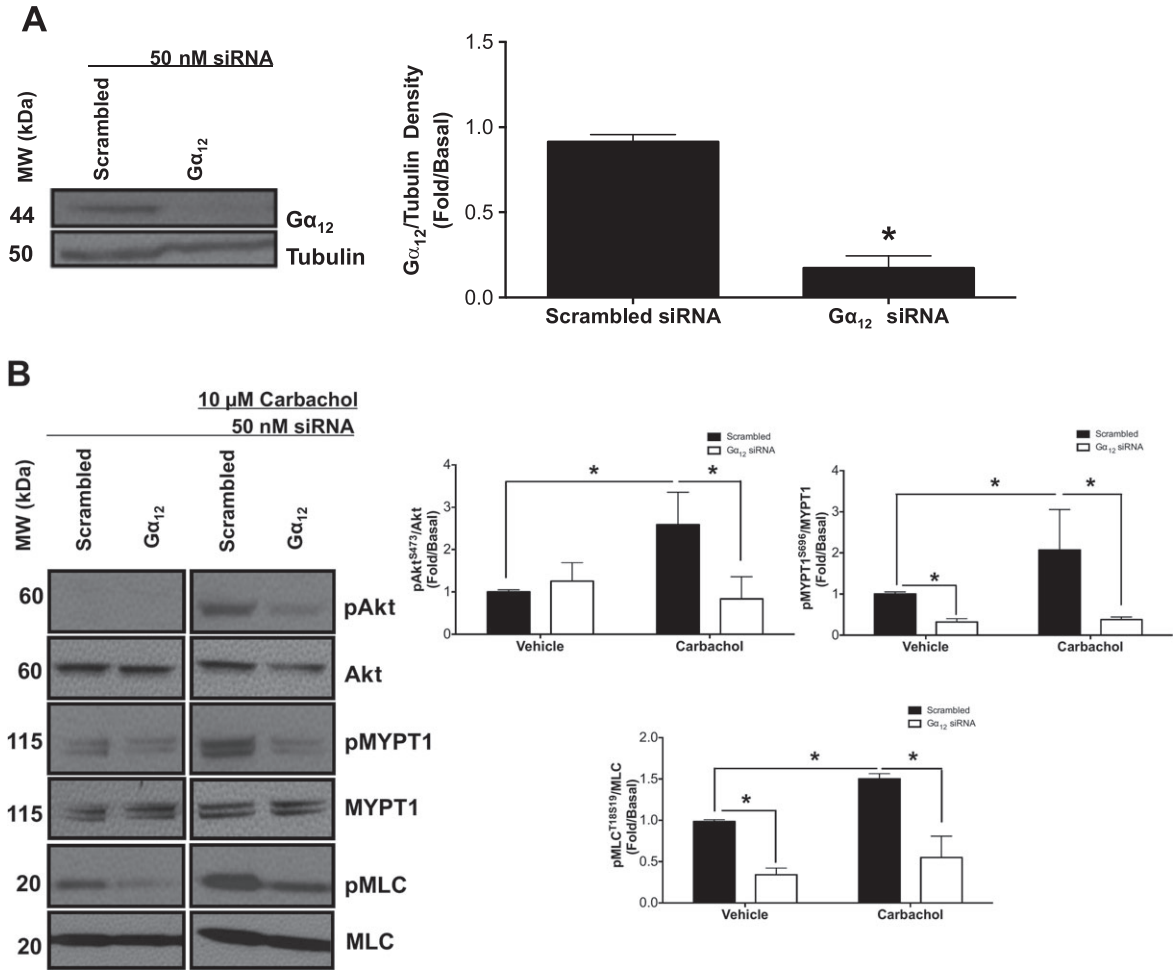

Figure 3

Effects of $G\alpha_{12}$ siRNA and p115RhoGEF-RGS overexpression on M_3 receptor-mediated activation of the PI3K/ROCK/MLC axis in HASMCs. (A–C) Measurement of phosphorylation responses to carbachol (10 μM, 10 min) and protein expression in primary HASMCs after transfection with $G\alpha_{12}$ or scrambled siRNA (50 nM, 72 h post-transfection). (A) Effect of $G\alpha_{12}$ or scrambled siRNA on protein expression. Data normalized to tubulin expression in the same samples. (B) Effect of carbachol on Akt, MYPT1 and MLC phosphorylation at S473 (pAkt), T696 (pMYPT1) and S19 (pMLC) after transfection with $G\alpha_{12}$ or scrambled siRNA. pAkt, pMYPT1 and pMLC data were normalized to total Akt (Akt), total MYPT1 (MYPT1) and total MLC (MLC). (C) Effect of p115RhoGEF-RGS overexpression on carbachol-induced Akt phosphorylation in hTERT-immortalized HASMCs. Control refers to hTERT-immortalized HASMCs that underwent G418 selection. (D) Effect of p115RhoGEF-RGS overexpression on carbachol-induced intracellular calcium mobilization in hTERT-immortalized HASMCs. Data are expressed as fold change over untreated (basal) samples that were measured on the same gel or plate. Data (means ± SD) are from five independent donors (n = 5). (E) Effect of p115RhoGEF-RGS overexpression on carbachol-induced contraction as measured by MTC analysis in hTERT-immortalized HASMCs (control, n = 278; p115RhoGEF-RGS, n = 237). (F) Representative images of a typical modified HASMC responding to carbachol. A single nucleus confirms the presence of one cell. The addition of carbachol induces increased force generation by the cell onto the contractible fluorescent micro-pattern, resulting in a smaller pattern over time. The white outline in the rightmost figure depicts the initial area of the cell before carbachol stimulation. (G) Quantification of cell contraction to carbachol in p115RhoGEF-RGS-expressing and control HASMCs. Line plots depict the evolution of contractile forces, shown as the median population-wide responsiveness in each of 36 technical experimental replicates (thin grey lines) and their mean (heavy lines) for both the p115RhoGEF-RGS-expressing and control HASMCs. Comparison of the heavy lines in the rightmost figure demonstrates a significant inhibition in contractile responsiveness in p115RhoGEF-RGS-expressing HASMCs compared with control HASMCs. Bars represent SEM, with each thin grey line representing between 13 and 52 isolated cells analysed per replicate, corresponding to ≥800 total cells analysed per condition. Data (means ± SEM) are from five biological replicates (n = 5). *$P < 0.05$, significantly different as indicated; in A, D, E unpaired t-test: in B, C, G, one-way ANOVA with Bonferroni's post test. Control in all experiments refers to hTERT-immortalized HASMCs that underwent G418 selection. n.s., not significant; RFU, relative fluorescence unit.

pharmacological inhibition of RhoA blunted carbachol-mediated activation of PI3K and that RhoA inhibitors induced dilation of hPCLS, suggesting that RhoA acts as an important mediator of airway tone.

Despite its lower expression levels, investigators suggest that the $G\alpha_q$-coupled M_3 receptor, and not the $G\alpha_i$-coupled M_2 muscarinic receptor, is the primary subtype responsible for bronchial and tracheal smooth muscle contraction (Roffel

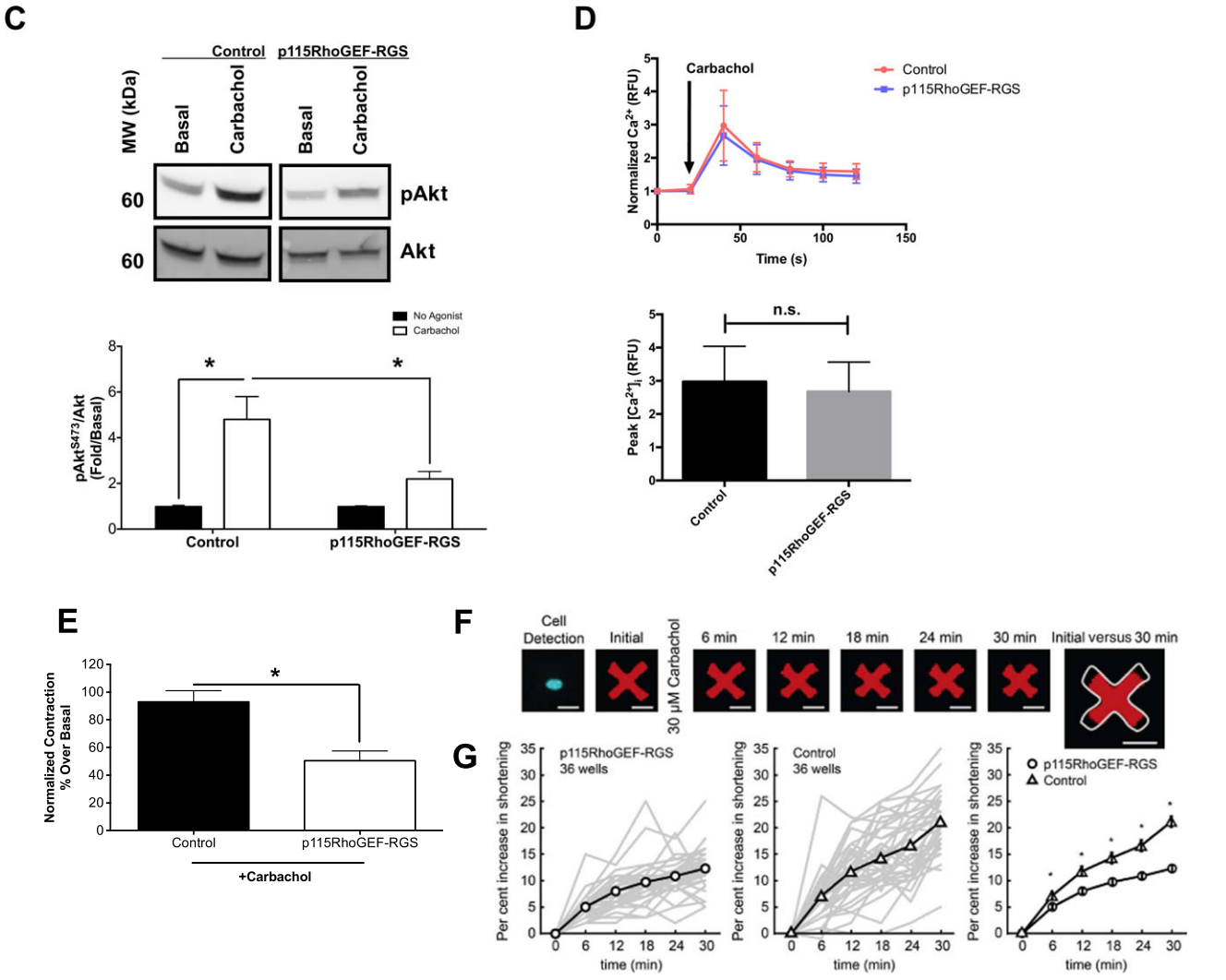

Figure 3
(Continued)

et al., 1988, 1990; Van Nieuwstadt *et al.*, 1997; Murthy *et al.*, 2003; Fisher *et al.*, 2004). Nonetheless, some studies suggest a role for M_2 receptors in mediating airway smooth muscle contraction in the peripheral airways (Roffel *et al.*, 1993; Struckmann *et al.*, 2003). Our findings using siRNA against the M_2 and M_3 receptors, as well as PTX to inactivate M_2 receptor-coupled $G\alpha_i$, demonstrated that the M_3 receptors are the dominant receptors mediating the activation of the PI3K/ROCK axis (Figure 1). Incubation with the siRNA for M_2 receptors surprisingly resulted in a robust activation of PI3K that possibly could be related to compensatory expression of proteins that activate PI3K (Murthy *et al.*, 2003). Our data stand in contrast with studies conducted in rabbit intestinal smooth muscle, where the M_2 receptors, through $G\beta\gamma$-dependent signalling activates PI3K (Murthy *et al.*, 2003). Interestingly, these cells expressed the p110γ isoform of PI3K that is not expressed in the HASMCs used in our studies (Goncharova *et al.*, 2002; Jude *et al.*, 2012; Himes *et al.*, 2015; Koziol-White *et al.*, 2016). $G\beta\gamma$ proteins are typically thought to signal to the p110γ isoforms of PI3K, not the p110α, p110β or p110δ isoforms expressed in our HASMCs (Leopoldt *et al.*, 1998). This illustrates an important concept that the identical receptors mediate signalling that is tissue and species specific.

GPCR-mediated activation of PI3K can occur through EGF receptor transactivation (Wang, 2016). Our previous studies, however, have demonstrated a lack of EGF receptor phosphorylation induced by carbachol in HASMCs (Krymskaya *et al.*, 2000).

As $G\alpha_{12/13}$ family proteins have been shown to modulate RhoA/ROCK pathways in other cell types, we used co-immunoprecipitation and SRE-luciferase reporter expressing HASMCs to demonstrate whether M_3 receptors coupled to $G\alpha_{12}$ in HASMCs (Figure 2). Our results suggest that M_3 receptors were indeed coupled to $G\alpha_{12}$ in HASMCs and that M_3 receptor-induced activation of $G\alpha_{12}$ was attenuated by

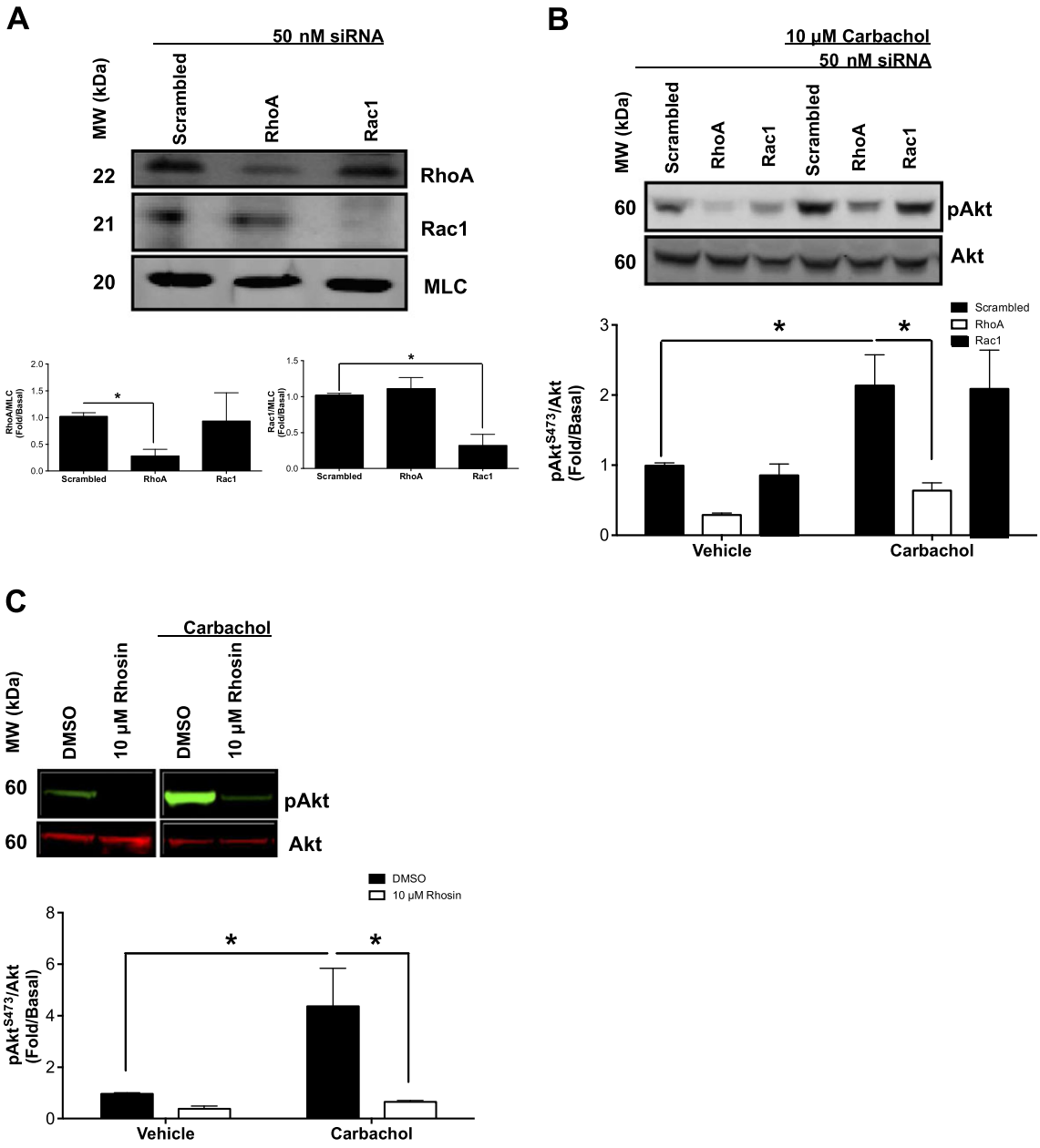

Figure 4

Effects of RhoA inhibitors and siRNA on M_3 receptor-mediated activation of PI3K in primary HASMCs. Measurement of phosphorylation responses to carbachol (10 μM, 10 min) and protein expression in primary HASMCs after transfection with RhoA, Rac1 or scrambled siRNA (50 nM, 72 h post-transfection) or after incubation with Rhosin (RhoA inhibitor) (10 μM, 30 min). (A) Effect of scrambled, RhoA and Rac1 siRNA on protein expression. Data normalized to MLC expression in the same samples. (B) Effect of carbachol on Akt phosphorylation at S473 (pAkt) after transfection with RhoA, Rac1 or scrambled siRNA. pAkt data were normalized to total Akt (Akt). (C) Effect of Rhosin on carbachol-induced Akt phosphorylation at S473 (pAkt). Data are expressed as fold change over untreated (basal) samples that were measured on the same gel. Data (means ± SD) are from five independent experiments ($n = 5$). *$P < 0.05$, significantly different as indicated; one-way ANOVA with Bonferroni's post test.

overexpression of the p115RhoGEF-RGS domain. Furthermore, $G\alpha_{12}$ siRNA attenuated carbachol-induced Akt, MYPT1 and MLC phosphorylation suggesting for the first time that $G\alpha_{12}$ regulates PI3K/ROCK axis activation and MLC phosphorylation in HASMCs. These data agree with previous studies demonstrating M_3 receptor-$G\alpha_{12}$ coupling in HEK293 cells (Rümenapp *et al.*, 2001). Although other studies have suggested a lack of M_3 receptor-$G\alpha_{12}$ coupling in murine airway smooth muscle. this discrepancy may reflect species differences between mice and humans. Our data highlight the importance and necessity of $G\alpha_{12}$ proteins in maintaining HASMC tone through pathways involving the PI3K-ROCK axis.

In order to determine whether $G\alpha_{12}$-mediated activation of the PI3K-ROCK axis involved RhoA, we used RhoA siRNA and Rhosin, a novel rationally designed inhibitor of RhoA

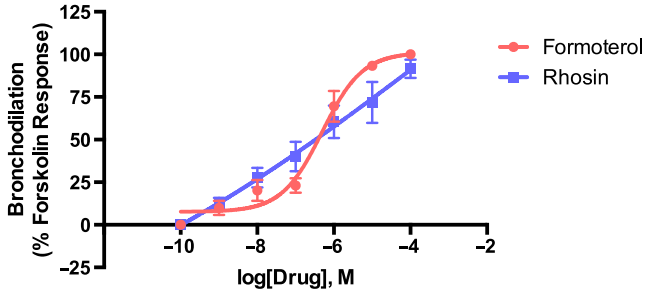

Figure 5

RhoA inhibition reverses carbachol-induced bronchoconstriction in a dose-dependent manner in hPCLS. Measurement of bronchodilation concentration–response to Rhosin in hPCLS. Airways were preconstricted with carbachol (10^{-8}–10^{-4} M) before dilation with Rhosin or formoterol (10^{-10}–10^{-4} M). Data were normalized to forskolin stimulation (10 μM) that was given after the final dose of formoterol or Rhosin. Each data point is expressed as mean ± SEM. Each group contains two airways from each of the three donors (total of six airways).

(Shang *et al.*, 2012), to test whether limiting RhoA signalling would attenuate PI3K activation. Our data showed that RhoA siRNA and inhibitors attenuated carbachol-induced Akt phosphorylation, suggesting PI3K as a novel intermediate in $G\alpha_{12}$ signalling. One study has suggested that Rho family GTPases and PI3K function cooperatively and that small GTPases can directly activate PI3K through a Rho binding domain on the p110 catalytic subunit. These findings offer an explanation for their relationship in $G\alpha_{12}$ signalling (Yang *et al.*, 2012). Further studies are warranted to study cooperativity in HASMCs. A limitation of our data is that the moderate potency of Rhosin allows the possibility of off-target effects at higher concentrations of Rhosin required. Our RhoA siRNA data, however, support the idea that $G\alpha_{12}$-mediated activation of PI3K is RhoA dependent.

We demonstrated using hPCLS that RhoA inhibition by Rhosin induced bronchodilation comparable with formoterol, a standard bronchodilator drug, suggesting that inhibition of our newly established $G\alpha_{12}$-mediated signalling pathway could provide a novel therapeutic strategy for bronchodilation in asthma.

Our current study and other studies have shown that there are a wide range of signalling pathways, kinases and scaffold proteins regulating ROCK activation in HASMCs including those involving arrestins, Src-family kinases, $G\alpha_{12}$ and PI3K (Pera *et al.*, 2015; Shaifta *et al.*, 2015; Bradley *et al.*, 2016; Koziol-White *et al.*, 2016). The many intermediates required for ROCK activation suggest the existence of signalling complexes driving ROCK activation. These complexes are composed of multiple kinases and scaffold proteins and warrant further investigation for several reasons. Their complexity and arrangement are highly cell and tissue specific. Targeting individual signalling intermediates such as kinases has limitations as they are often ubiquitously expressed, allowing for toxicities and side effects, even with inhaled delivery systems. Targeting signalling complex formation would provide greater tissue specificity for therapeutics. Furthermore, using combinations of therapeutic agents to target constituents of ROCK signalling complexes allows the potential for combination therapies with lower doses of each individual drug. This would allow improved efficacy with fewer side effects and could provide for improved bronchodilators.

In summary, our data have demonstrated a novel coupling of M_3 receptors to $G\alpha_{12}$ HASMCs and that $G\alpha_{12}$ plays a crucial role in contraction through RhoA-dependent activation of the PI3K/ROCK axis. We have shown that inhibition of RhoA induces bronchodilation in hPCLS and that targeting $G\alpha_{12}$ signalling may provide novel therapeutic targets in asthma.

Acknowledgements

We would like to thank Philip Wedegaertner for providing the p115RhoGEF-RGS construct.

This study is supported by the National Heart, Lung, and Blood Institute P01-HL114471 (R.A.P./S.S.A./R.B.P.), HL58506 (R.B.P.) and 1F31HL134264 (E.J.Y.).

Author contributions

E.J.Y., G.C., C.J.K.W., J.V.M., R.B.P., S.S.A., D.D.C. and R.A.P. J. contributed to the experimental design. E.J.Y., G.C., C.J.K. W., H.L., C.A.O., J.A.J., I.P., R.D. and K.S. performed the experiments and analysed the data. E.J.Y. wrote the manuscript. E.J.Y., R.B.P., S.S.A. and R.A.P.J. edited the manuscript.

Conflict of interest

The authors declare no conflicts of interest.

Declaration of transparency and scientific rigour

This Declaration acknowledges that this paper adheres to the principles for transparent reporting and scientific rigour of preclinical research recommended by funding agencies, publishers and other organisations engaged with supporting research.

References

Alexander SPH, Davenport AP, Kelly E, Marrion N, Peters JA, Benson HE *et al.* (2015a). The Concise Guide to PHARMACOLOGY 2015/16: G protein-coupled receptors. Br J Pharmacol 172: 5744–5869.

Alexander SPH, Fabbro D, Kelly E, Marrion N, Peters JA, Benson HE *et al.* (2015b). The Concise Guide to PHARMACOLOGY 2015/16: Enzymes. Br J Pharmacol 172: 6024–6109.

Alexander SPH, Kelly E, Marrion N, Peters JA, Benson HE, Faccenda E *et al.* (2015c). The Concise Guide to PHARMACOLOGY 2015/16: Other proteins. Br J Pharmacol 172: 5734–5143.

Amrani Y, Tliba O, Deshpande DA, Walseth TF, Kannan MS, Panettieri RA (2004). Bronchial hyperresponsiveness: insights into new signaling molecules. Curr Opin Pharmacol 4: 230–234.

An SS, Fabry B, Trepat X, Wang N, Fredberg JJ (2006). Do biophysical properties of the airway smooth muscle in culture predict airway hyperresponsiveness? Am J Respir Cell Mol Biol 35: 55–64.

Balenga N a, Klichinsky M, Xie Z, Chan EC, Zhao M, Jude J *et al.* (2015). A fungal protease allergen provokes airway hyper-responsiveness in asthma. Nat Commun 6: 6763.

Billington CK, Penn RB (2002). M3 muscarinic acetylcholine receptor regulation in the airway. Am J Respir Cell Mol Biol 26: 269–272.

Billington CK, Penn RB (2003). Signaling and regulation of G protein-coupled receptors in airway smooth muscle. Respir Res 4: 2.

Black JL, Panettieri RA, Banerjee A, Berger P (2012). Airway smooth muscle in asthma. Just a target for bronchodilation? Clin Chest Med 33: 543–558.

Bradley SJ, Wiegman CH, Iglesias MM, Kong KC, Butcher AJ, Plouffe B *et al.* (2016). Mapping physiological G protein-coupled receptor signaling pathways reveals a role for receptor phosphorylation in airway contraction. Proc Natl Acad Sci U S A 113: 4524–4529.

Chiba Y, Misawa M (2001). Increased expression of G_{12} and G_{13} proteins in bronchial smooth muscle of airway hyperresponsive rats. Inflamm Res 50: 333–336.

Chiba Y, Misawa M (2004). The role of RhoA-mediated Ca^{2+} sensitization of bronchial smooth muscle contraction in airway hyperresponsiveness. J Smooth Muscle Res 40: 155–167.

Chiba Y, Matsusue K, Misawa M (2010). RhoA, a possible target for treatment of airway hyperresponsiveness in bronchial asthma. J Pharmacol Sci 114: 239–247.

Cooper PR, Lamb R, Day ND, Branigan PJ, Kajekar R, San Mateo L *et al.* (2009). TLR3 activation stimulates cytokine secretion without altering agonist-induced human small airway contraction or relaxation. Am J Physiol - Lung Cell Mol Physiol 297: L530–L537.

Curtis MJ, Bond RA, Spina D, Ahluwalia A, Alexander SP, Giembycz MA *et al.* (2015). Experimental design and analysis and their reporting: new guidance for publication in BJP. Br J Pharmacol 172: 3461–3471.

Deshpande DA, Yan H, Kong K-C, Tiegs BC, Morgan SJ, Pera T*et al.* (2014). Exploiting functional domains of GRK2/3 to alter the competitive balance of pro- and anticontractile signaling in airway smooth muscle. FASEB J 28: 956–965.

Fabry B, Maksym GN, Butler JP, Glogauer M, Navajas D, Fredberg JJ (2001). Scaling the microrheology of living cells. Phys Rev Lett 87: 148102.

Fisher JT, Vincent SG, Gomeza J, Yamada M, Wess J (2004). Loss of vagally mediated bradycardia and bronchoconstriction in mice lacking M_2 or M_3 muscarinic acetylcholine receptors. FASEB J 18: 711–713.

Goncharova EA, Ammit AJ, Irani C, Carroll RG, Eszterhas AJ, Panettieri RA *et al.* (2002). PI3K is required for proliferation and migration of human pulmonary vascular smooth muscle cells. Am J Physiol Lung Cell Mol Physiol 283: L354–L363.

Himes BE, Koziol-White C, Johnson M, Nikolos C, Jester W, Klanderman B *et al.* (2015). Vitamin D modulates expression of the airway smooth muscle transcriptome in fatal asthma. PLoS One 10: e0134057.

Jude JA, Tirumurugaan KG, Kang BN, Panettieri RA, Walseth TF, Kannan MS (2012). Regulation of CD38 expression in human airway smooth muscle cells: role of class I phosphatidylinositol 3 kinases. Am J Respir Cell Mol Biol 47: 427–435.

Kong KC, Gandhi U, Martin TJ, Anz CB, Yan H *et al.* (2008). Endogenous Gs-coupled receptors in smooth muscle exhibit differential susceptibility to GRK2/3-mediated desensitization. Biochemistry 47: 9279–9288.

Koziol-White CJ, Panettieri RA (2011). Airway smooth muscle and immunomodulation in acute exacerbations of airway disease. Immunol Rev 242: 178–185.

Koziol-White CJ, Yoo EJ, Cao G, Zhang J, Papanikolaou E, Pushkarsky I *et al.* (2016). Inhibition of phosphoinositide 3-kinase (PI3K) promotes bronchodilation of human small airways in a Rho kinase-dependent manner. Br J Pharmacol 173: 2726–2738.

Krymskaya VP, Orsini MJ, Eszterhas AJ, Brodbeck KC, Benovic JL, Panettieri RA *et al.* (2000). Mechanisms of proliferation synergy by receptor tyrosine kinase and G protein-coupled receptor activation in human airway smooth muscle. Am J Respir Cell Mol Biol 23: 546–554.

Lee SJ, Lee WH, Ki SH, Kim YM, Lee SJ, Lee CH *et al.* (2009). Gα13 regulates methacholine-induced contraction of bronchial smooth muscle via phosphorylation of MLC20. Biochem Pharmacol 77: 1497–1505.

Leopoldt D, Hanck T, Exner T, Maier U, Wetzker R, Nürnberg B (1998). Gbg stimulates phosphoinositide 3-kinase-g by direct interaction with two domains of the catalytic p110 subunit. JBiolChem 273: 7024–7029.

Murthy KS, Zhou H, Grider JR, Brautigan DL, Eto M, Makhlouf GM (2003). Differential signalling by muscarinic receptors in smooth muscle: m2-mediated inactivation of myosin light chain kinase via Gi3, Cdc42/Rac1 and p21-activated kinase 1 pathway, and m3-mediated MLC20 (20 kDa regulatory light chain of myosin II) phosphorylat. Biochem J 374: 145.

Panettieri RA (2016). Neutrophilic and pauci-immune phenotypes in severe asthma. Immunol Allergy Clin North Am 36: 569–579.

Panettieri RA, Murray RK, DePalo LR, Yadvish PA, Kotlikoff MI (1989a). A human airway smooth muscle cell line that retains physiological responsiveness. Am J Physiol 256: C329–C335.

Panettieri RA, Murray RK, DePalo LR, Yadvish PA, Kotlikoff MI (1989b). A human airway smooth muscle cell line that retains physiological responsiveness. Am J Physiol 256: C329–C335.

Penn RB, Benovic JL (2008). Regulation of heterotrimeric G protein signaling in airway smooth muscle. Proc Am Thorac Soc 5: 47–57.

Pera T, Penn RB (2016). Bronchoprotection and bronchorelaxation in asthma: new targets, and new ways to target the old ones. Pharmacol Ther 164: 82–96.

Pera T, Hegde A, Deshpande DA, Morgan SJ, Tiegs BC, Theriot BS *et al.* (2015). Specificity of arrestin subtypes in regulating airway smooth muscle G protein-coupled receptor signaling and function. FASEB J Off Publ Fed Am Soc Exp Biol 29: 4227–4235.

Riobo NA, Manning DR (2005). Receptors coupled to heterotrimeric G proteins of the G_{12} family. Trends Pharmacol Sci 26: 146–154.

Roffel AF, Elzinga CRS, Amsterdam RGMV, Zeeuw RAD, Zaagsma J (1988). Muscarinic M2 receptors in bovine tracheal smooth muscle: discrepancies between binding and function. Eur J Pharmacol 153: 73–82.

Roffel AF, Elzinga CR, Zaagsma J (1990). Muscarinic M3 receptors mediate contraction of human central and peripheral airway smooth muscle. Pulm Pharmacol 3: 47–51.

Roffel AF, Elzinga CRS, Zaagsma J (1993). Cholinergic contraction of the guinea pig lung strip is mediated by muscarinic M2-like receptors. Eur J Pharmacol 250: 267–279.

Rümenapp U, Asmus M, Schablowski H, Woznicki M, Han L, Jakobs KH *et al*. (2001). The M3 muscarinic acetylcholine receptor expressed in HEK-293 cells signals to phospholipase D via G_{12} but not Gq-type G proteins. Regulators of G proteins as tools to dissect pertussis toxin-resistant G proteins in receptor-effector coupling. J Biol Chem 276: 2474–2479.

Shaifta Y, Irechukwu N, Prieto-Lloret J, Mackay CE, Marchon KA, Ward JPT *et al*. (2015). Divergent modulation of Rho-kinase and Ca^{2+} influx pathways by Src family kinases and focal adhesion kinase in airway smooth muscle. Br J Pharmacol 172: 5265–5280.

Shang X, Marchioni F, Sipes N, Evelyn CR, Jerabek-Willemsen M, Duhr S *et al*. (2012). Rational design of small molecule inhibitors targeting RhoA subfamily Rho GTPases. Chem Biol 19: 699–710.

Siehler S (2009). Regulation of RhoGEF proteins by $G_{12/13}$-coupled receptors. Br J Pharmacol 158: 41–49.

Southan C, Sharman JL, Benson HE, Faccenda E, Pawson AJ, Alexander SPH *et al*. (2016). The IUPHAR/BPS Guide to PHARMACOLOGY in 2016: towards curated quantitative interactions between 1300 protein targets and 6000 ligands. Nucl Acids Res 44: D1054–D1068.

Struckmann N, Schwering S, Wiegand S, Gschnell A, Yamada M, Kummer W*et al*. (2003). Role of muscarinic receptor subtypes in the constriction of peripheral airways: studies on receptor-deficient mice. Mol Pharmacol 64: 1444–1451.

Tseng P, Pushkarsky I, Di Carlo D (2014). Metallization and biopatterning on ultra-flexible substrates via dextran sacrificial layers. PLoS One 9 (8) e106091.

Van Nieuwstadt RA, Henricks PA, Hajer R, van der Meer van Roomen WA, Breukink HJ, Nijkamp FP (1997). Characterization of muscarinic receptors in equine tracheal smooth muscle in vitro. Vet Q 19: 54–57.

Wang Z (2016). Transactivation of epidermal growth factor receptor by G protein-coupled receptors: recent progress, challenges and future research. Int J Mol Sci 17: 95.

Wells CD, Liu MY, Jackson M, Gutowski S, Sternweis PM, Rothstein JD *et al*. (2002). Mechanisms for reversible regulation between G_{13} and Rho exchange factors. J Biol Chem 277: 1174–1181.

Worzfeld T, Wettschureck N, Offermanns S (2008). G_{12}/G_{13}-mediated signalling in mammalian physiology and disease. Trends Pharmacol Sci 29: 582–589.

Yang HW, Shin MG, Lee S, Kim JR, Park WS, Cho KH *et al*. (2012). Cooperative activation of PI3K by Ras and Rho family small GTPases. Mol Cell 47: 281–290.

Supporting Information

Additional Supporting Information may be found online in the supporting information tab for this article.

https://doi.org/10.1111/bph.14040

Figure S1 Uncropped immunoblot from Figure 2A.